Experimental control of pattern formation by photonic lattices

N. Marsal[1], D. Wolfersberger[1], M. Sciamanna[1], G. Montemezzani[1], D. N. Neshev[2]

[1] *Laboratoire Matériaux Optiques, Photoniques et Systèmes (LMOPS), CNRS UMR 7132, Unité de recherche commune à Supelec et Université Paul Verlaine de Metz, France*

[2] *Nonlinear Physics Centre, Research School of Physical Sciences and Engineering, Australian National University, Canberra, 0200 ACT, Australia*

Compiled September 25, 2008

We study the control of modulational instability and pattern formation in a nonlinear dissipative feedback system with a periodic modulation of the material refractive index. We use an one-dimensional photonic lattice in a single-mirror feedback configuration and identify three mechanisms for pattern control: band-gap suppression of instability modes, periodicity induced pattern modes, and orientational pattern control.

OCIS codes: 190.4420, 190.3100

Nonlinear systems displaying patterns are ubiquitous in nature [1] and experience similar properties due to the unique interplay between nonlinearity, dispersion, gain, loss, and feedback in the system. In general such dissipative systems display a large number of unstable pattern modes, which are related to the breaking of the rotational and translational symmetry. Due to the feedback however, only few of these modes are normally excited.

In optics, the formation of patterns in cavities is widely studied [2–6] due to possible applications in emission control of large-mode-area lasers. In these studies, various techniques for control of the pattern formation have been reported. These include methods based on spatial filtering [2], frequency detuning [3], and spatial seeding of nonlinear modes [4, 5]. In addition, theoretical predictions have demonstrated the extended ability for control of the pattern formation by implementation of a photonic periodic structure inside the cavity [7]. Indeed, the use of periodic structures have proven to enable manipulation of the fundamental aspects of wave propagation [8] and the implementation of such structures inside a cavity can lead to novel nonlinear phenomena, including discrete cavity modulational instability (MI) [7] and discrete cavity solitons [9]. It was also shown experimentally that a periodic structure can lead to suppression of the longitudinal dynamic instability for counter-propagating spatial solitons [10]. Despite the large theoretical interest however, an experimental demonstration of the interplay between periodic photonic bandgap structure and optical patterns in a feedback system is, to the best of our knowledge, still lacking.

In this Letter, we study experimentally the conditions for pattern formation in a feedback nonlinear system with an one-dimensional (1D) periodically modulated refractive index. We combine two concepts: a photorefractive two-wave mixing in a single-mirror configuration [3] and an optically induced lattice [11]. We study how the strength and periodicity of the optical lattice influence the conditions for MI, and correspondingly the pattern formation. By properly adjusting the optical lattice wavevectors with respect to the wavevectors of the system instability modes, we demonstrate three important control mechanisms: (i) band-gap inhibition of instability modes; (ii) seeding of instability patterns by the lattice periodicity; and (iii) lattice-induced pattern reorientation.

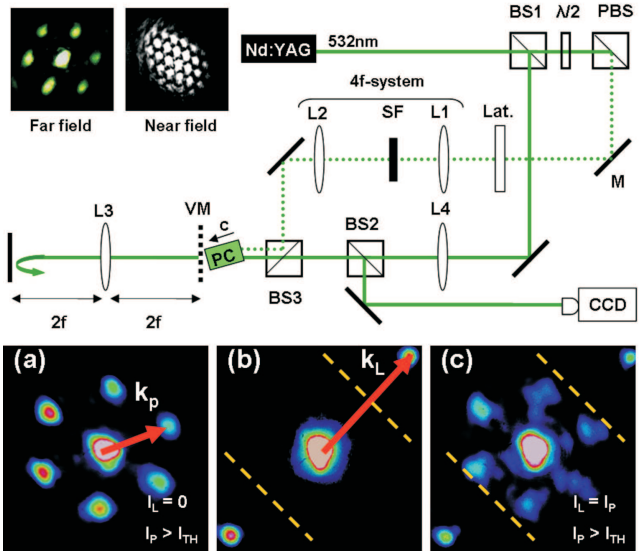

Fig. 1. Top: Experimental setup. L - lenses, PBS - polarising beam splitter, SF - spatial filter, Lat - 1D transmission grating, $\lambda/2$ - half-wave plate, M - mirror, VM - virtual mirror, PC - $BaTiO_3$ photorefractive crystal. Inset: typical far- and near-field patterns. Bottom: Far-field patterns: (a) hexagonal pattern without optical lattice, (b) linear diffraction on the optical lattice, (c) coexistence between nonlinear optical pattern and linear diffraction for $k_L \simeq 2.2 k_P$. Dashed lines denote the position of the lattice bandgap.

In our experiments we employ the setup shown in Fig. 1. The part of the setup indicated by the solid line is similar to the configuration described in Ref. [2]. It

contains a photorefractive two-wave mixing in a reflection grating geometry and a tunable single feedback. In this counterpropagating configuration, the laser beam becomes unstable against MI and sidebands arranged in hexagonal patterns grow from scattered light appearing from this geometry. Their directions are determined by both the phase matching in the nonlinear gain medium and the effect of diffraction introduced by the feedback. A lot of transverse k-vectors can appear but only the one with the minimal gain threshold will grow [12, 13]. Experimentally, we use a p-polarized 532 nm pattern beam that is focused inside an undoped $BaTiO_3$ crystal to a 400 μm diameter. The crystalline c-axis points towards the feedback mirror, but is rotated by roughly 25° with respect to the optical axis of the system. The resulting contribution of the large electro-optic coefficient r_{232} in the conventionally hole-conducting $BaTiO_3$ allows to switch the sign of the photorefractive gain for the backward propagating beam from negative to positive [14]. The feedback is generated via a mirror placed behind the lens L3. The mirror can be precisely moved longitudinally, to vary the position of the corresponding virtual mirror (Fig. 1). This allows to adjust positive or negative effective propagation lengths [2]. Depending on the distance mirror-crystal and above a threshold intensity (I_{TH}) a finite set of wave vectors pairs is selected, leading to formation of hexagonal pattern with a typical far- and near-field (I_P) intensity distributions shown in the inset of Fig. 1(top).

To create a periodic optical lattice, a Gaussian lattice beam (shown with a dotted line in Fig. 1) is sent through a 1D transmission grating with variable periodicity. The ±1st diffraction orders are then selected by a spatial filter in the Fourier plane of the lens L1 and recombined in the crystal by a $4f$ system [10]. The intensity of the lattice beam (I_L) is tuned thanks to a half-wave plate and a polarizing beam splitter. The patterns are identified by monitoring their far-field onto a CCD camera. In order to avoid coherent interactions between pattern and lattice beams, they are orthogonally polarized.

Figure 1(a) shows the typical far-field hexagonal pattern formed in the absence of the lattice beam. The optical power of the pattern beam necessary to reach the hexagonal pattern threshold is 20 mW. To test the strength of the optical lattice we temporarily remove the feedback mirror and monitor the far-field of the pattern beam diffracted on the optical lattice. The pattern beam diffraction gives rise to the two outer spots appearing along the diagonal, corresponding to the 45° lattice orientation, as seen in Fig. 1(b). The central spot corresponds to the zero-order of diffraction, and the other two spots to the ±1 diffraction orders. The arrows in Fig. 1(a,b) represent the transverse wavevectors associated with the hexagonal pattern ($\boldsymbol{k}_P$) and the optical lattice ($\boldsymbol{k}_L$). The former corresponds to the spontaneous transverse k-vector of the reflection grating that arises during pattern formation [13]. The dashed lines in Figs. (1–3) represent the position of the bandgap of the photonic lattice, situated at $k_L/2$ and corresponding to the edges of the first Brillouin zone [15].

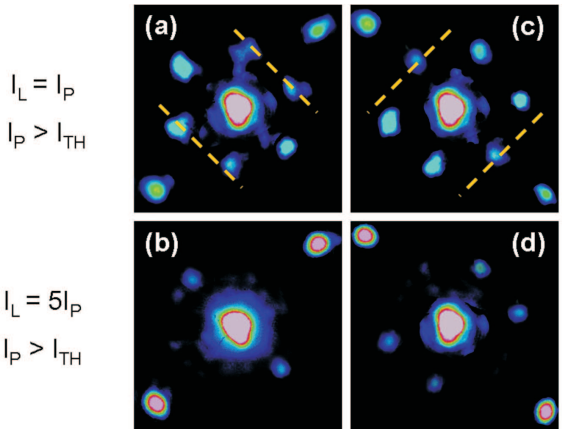

Fig. 2. Bandgap inhibition of instability modes for two different lattice beam intensities. (a, b) Suppression of instability modes for $k_L \simeq \sqrt{3} k_P$. (c, d) Suppression of instability modes when $k_L \simeq 2k_P$ in perpendicular direction. Dashed lines indicate the edges of Brillouin zone.

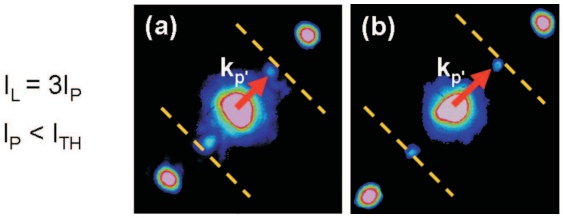

Fig. 3. Seeding of instability modes. Diagonal pattern obtained at intensity below the hexagon formation threshold with (a) $k_L \simeq 1.3 k_{P(hexagons)}$ and (b) $k_L \simeq 2.2 k_{P(hexagons)}$. $k_{P'}$ is the new wavevector associated with the new diagonal pattern.

In the following, we investigate the effect of the relative magnitude and orientation of k_L on the formation of optical patterns in the system. In the experiments we first send the lattice beam into the photorefractive crystal to create the periodic refractive index modulation and then the pattern beam is launched into the medium. For $k_L \simeq 2.2 k_P$ [Fig. 1(c)], when all the wavevectors of the instability modes fall within the first Brillouin zone of the lattice, the nonlinear optical hexagonal pattern co-exists with the linear 1D diffraction. Note that in this case the optical power of the pattern beam (≃30 mW) was larger than the previous value of 20 mW, because the presence of the optical lattice in the crystal tends to increase the hexagonal pattern threshold.

An important configuration for bandgap control of the optical patterns is the one where the periodicity of the optical lattice is such that $k_L = \sqrt{3} k_P$. In this case, some spots of the hexagonal pattern are situated exactly in the bandgap region of the optical lattice [Fig. 2(a)], pattern and lattice beams intensities being comparable. By increasing the lattice beam intensity, $I_L = 5 I_P$ [as seen by the two brighter outer spots in Fig. 2(b) than in Fig. 2(a)], the MI can be suppressed in the bandgap

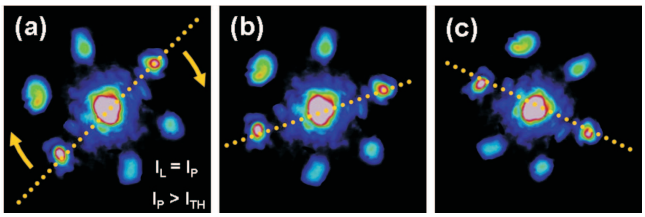

Fig. 4. Pattern orientation control. From left to right, pattern orientation following the lattice rotation. Dotted lines indicate the optical lattice position, the arrows – the rotation of the lattice.

region [Fig. 2(b)] as a result of the fact that the lattice bandgap prohibits the growth from noise of instability modes with corresponding wavevectors. Qualitatively similar effect occurs if two spots of the hexagons overlap the bandgap area for $k_L \simeq 2k_P$ [Fig. 2(c, d)], again leading to symmetry breaking of the induced patterns. It is important to note that the output differs drastically, when the optical lattice is sent through the crystal after the formation of the hexagonal pattern. In this case, the established high intensity instability modes shift the lattice bandgaps such that the propagation constant of the modes lies outside the bandgap region and suppression of the instability is no longer possible.

The results above are obtained in a range of parameters for which the pattern beam dominates the dynamics. This situation can be changed if we decrease the pattern beam intensity below the threshold for the hexagon formation. In this case, we have found that the presence of the lattice periodicity can induce a new optical pattern solution that reflects the lattice geometry. We show an example of this in Fig. 3(a) where the pattern beam power was 15 mW. The new seeded pattern with wavevectors ($k_{P'}$ in Fig. 3) inside the first Brillouin zone now presents a diagonal symmetry instead of the hexagonal one and is animated by an oscillating dynamics. In other words, the optical lattice enables the appearance of a new wavevector whose gain is smaller than the one for the hexagons. Indeed, this diagonal pattern disappears in favour of a hexagonal one (with the previous wavevector $k_P \neq k_{P'}$) when the probe beam intensity is increased and reaches the threshold for the hexagons. Similar effects occur for any lattice periodicity [Fig. 3(b)]. Note that without feedback in the system, such diagonal solutions are not present.

Finally, we have considered the situation when the wavevectors corresponding to scattering from the optical lattice coincide with the wavevectors of the instability gain, $k_L \simeq k_P$ (see the two brighter spots located on the dotted line in Fig. 4). Similar to the previous case, when the pattern beam intensity is below the threshold for formation of hexagons, we observe the induced diagonal pattern. However, above this threshold and for an arbitrary direction of the lattice (dotted lines in Fig. 4), the hexagonal pattern becomes locked to the lattice orientation. By rotating the 1D lattice, we observe a continuous rotation of the hexagons following the lattice orientation [Fig. 4(b, c)]. This effect enables not only to choose an orientation for the hexagons but also to stabilize the otherwise rotationally unstable pattern. Note that, after switching off the lattice beam, the hexagons remain unchanged in their last position. This observation suggests that the orientation of the hexagonal pattern depends on the starting conditions of the system.

In conclusion, we have experimentally demonstrated a new method for controlling the pattern formation in a single feedback system that takes advantage of the presence of an optically induced photonic lattice. We demonstrate a suppression of the instability occurring when a part of the hexagonal pattern is situated in the bandgap region of the lattice. In addition, new symmetry patterns can be formed below the threshold for hexagon formation. A control of the hexagon orientation is also achieved when the lattice and pattern wavevectors have the same magnitude. To our knowledge, this work shows for the first time how a photonic lattice can influence the pattern formation in several fashions. We believe that similar manipulation of the nonlinear dynamics can be potentially observed in lasers with large-mode area and embedded photonic crystal structures.

The authors acknowledge the support of the Conseil Régional de Lorraine, the bilateral FAST program, and Australian Research Council through Discovery projects.

References

1. P. Manneville, Dissipative Structure and Weak Turbulence, Academic Press, San Diego (1990).
2. C. Denz, Ph. Jander, M. Schwab, Ann. Phys. (Leipzig) **13**, 391–402 (2004).
3. M. Schwab, C. Denz, A. V. Mamaev, M. Saffman, J. Opt. B **3**, 318–327 (2001).
4. C. Cleff, B. Gütlich, C. Denz, Phys. Rev. Lett. **100**, 233902(4) (2008).
5. R. Neubecker and A. Zimmermann, Phys. Rev. E **65**, 035205(4) (2002).
6. T. Carmon, M. Soljacic, and M. Segev, Phys. Rev. Lett. **89**, 183902(4) (2002).
7. D. Gomila, R. Zambrini, and G.-L. Oppo, Phys. Rev. Lett. **92**, 253904(4) (2004).
8. J. D. Joannopoulos, P. R. Villeneuve, and S. Fan, Nature **386**, 143–149 (1997).
9. U. Peschel, O. Egorov, and F. Lederer, Opt. Lett. **29**, 1909(3) (2004).
10. S. Koke, D. Träger, P. Jander, M. Chen, D. N. Neshev, W. Krolikowski, Yu. S. Kivshar, C. Denz, Opt. Express **15**, 6279(13) (2007).
11. N. K. Efremidis, S. Sears, D. N. Christodoulides, J. W. Fleischer, and M. Segev, Phys. Rev. E **66**, 046602(5) (2002).
12. G. D'Alessandro and W. J. Firth, Phys. Rev. Lett. **66**, 2597(4) (1991).
13. T. Honda, Opt. Lett. **18**, 598–560 (1993).
14. G. Montemezzani, Phys. Rev. A **62**, 053803(12) (2000).
15. C. Lou, X. Wang, J. Xu, and Z. Chen, Phys. Rev. Lett. **98**, 213903(4) (2007).